

# Colloidal Stability of Nanoparticles Stabilized with Mixed Ligands in Solvents with Varying Polarity

Hu Zhu,<sup>a</sup> Elizabeth Prince,<sup>a</sup> Pournima Narayanan,<sup>a</sup> Kun Liu,<sup>b,\*</sup> Zhihong Nie,<sup>\*c</sup>

Eugenia Kumacheva<sup>\*a,d,e,f</sup>

<sup>a</sup> Department of Chemistry, University of Toronto, 80 Saint George street, Toronto, Ontario M5S 3H6, Canada

<sup>b</sup> State Key Laboratory of Supramolecular Structure and Materials, College of Chemistry, Jilin University, Changchun 130012, PR China

<sup>c</sup> State Key Laboratory of Molecular Engineering of Polymers, Department of Macromolecular Science, Fudan University, Shanghai, 200438, PR China

\*Corresponding author. E-mail address: [eugenia.kumacheva@utoronto.ca](mailto:eugenia.kumacheva@utoronto.ca) (E.K.); [kliu@jlu.edu.cn](mailto:kliu@jlu.edu.cn) (K.L.); [znie@fudan.edu.cn](mailto:znie@fudan.edu.cn) (Z.N.)

## Experimental

**Materials.** Anhydrous tetrahydrofuran (THF, 99.9%, inhibitors-free), anhydrous *N,N*-dimethylformamide (DMF, 99.8%), gold(III) chloride hydrate (99.995%), hexadecyltrimethylammonium bromide (CTAB, >99%), sodium citrate dehydrate (>99%), sodium borohydride (>99%), and *L*-ascorbic acid (>99%) were purchased from MilliporeSigma.  $\omega$ -thiol-terminated polystyrene (PS,  $M_n=50$  kg/mol, PDI=1.06) was purchased from Polymer Source (Dorval, QC, Canada). All products were used as received. Deionized water (resistivity 18.2 M $\Omega$ ·cm; Milli-Q Reference Water Purification System) was used in all experiments. 20 mL scintillation vials were purchased from VWR and used without further cleaning.

**Synthesis of AuNPs.** The spherical AuNPs with targeted diameter of 20 nm were synthesized using a seed-mediated growth method reported elsewhere.<sup>1,2</sup> Briefly, the seeds were synthesized by reducing chloroauric acid with sodium borohydride in the presence of sodium citrate,

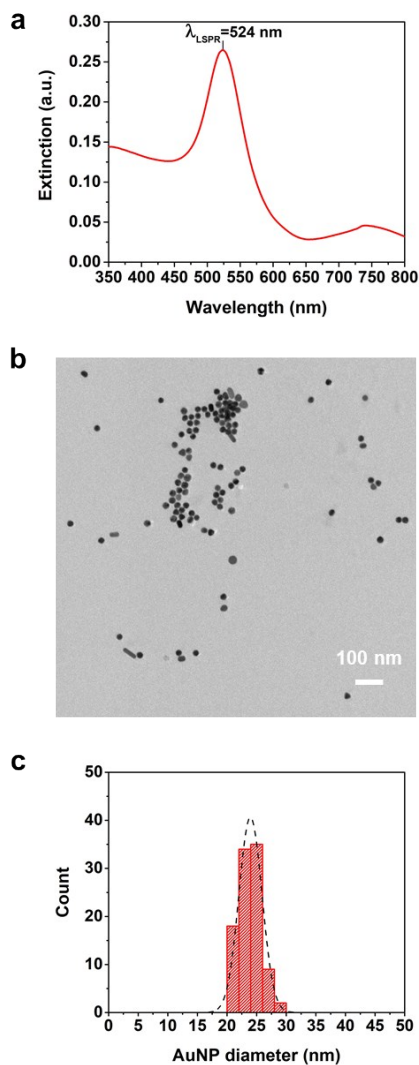
followed by the growth step using ascorbic acid as a reducing agent and CTAB as stabilizer. The obtained AuNPs were characterized by UV-vis and TEM (Figure S1).

**Ligand exchange.** The ligand exchange of CTAB with PS was carried out in THF. Typically, 1 mL of AuNP colloidal solution was concentrated to <50  $\mu$ L in a plastic centrifugation tube using centrifugation at 10000 *g* for 20 min at room temperature. After removing the supernatant, 0.5 mL of freshly prepared 0.5 mg/mL PS solution in THF was added to the concentrated AuNP solution under sonication. Note that CTAB-capped AuNPs do not disperse in THF, however they can be dispersed in the PS solution in THF under sonication. Following sonication, the solution was stored overnight in dark. Subsequently, the PS-grafted AuNPs were separated from free (nonattached) PS via 5 cycles of centrifugation (20000 *g*, 5 min, 20 °C), removal of the supernatant, and dilution of the solution with 1 mL THF. As both CTAB and PS are present on the AuNP surface after the ligand exchange process, we denoted the AuNPs as PS/CTAB-functionalized AuNPs, while the AuNPs prior to ligand exchange were denoted as CTAB-stabilized AuNPs.

**Colloidal stability and self-assembly of AuNPs.** The colloidal stability and self-assembly of CTAB- and CTAB/PS-functionalized AuNPs were controlled by changing the solvent polarity, that is, by using water/THF mixtures with different water content,  $C_w$ . To minimize kinetic effects, a small volume (0.5 mL) CTAB/PS-capped AuNP solution was added to a large volume (9.5 mL) of water/THF solvent in 20 mL scintillation vials under sonication to reach  $C_w$  in the range of 3-09 vol%. Subsequently, the solution was incubated for various time intervals (up to a month).

**Characterization of colloidal stability and self-assembly of AuNPs.** The photographs of AuNP solutions were taken using a Samsung Glaxy S9 cellphone. UV-visible spectra of AuNP solutions in a glass cuvette with 1.0 cm path length were collected using a Varian Cary 5000UV-Vis-NIR spectrophotometer. The hydrodynamic diameter and  $\zeta$ -potential of AuNPs were determined using a Malven Zetasizer Nano ZS instrument. Transmission electron microscopy (TEM) images were obtained using a Hitachi HD-2000 STEM with a working voltage at 80 kv and 200 kV. The samples for TEM imaging were prepared by depositing a small (~20  $\mu$ L) droplet of the AuNP solution on a 300 mesh carbon-coated copper grid and allowing the solvent to evaporate. The AuNP size distribution was analyzed using ImageJ software.

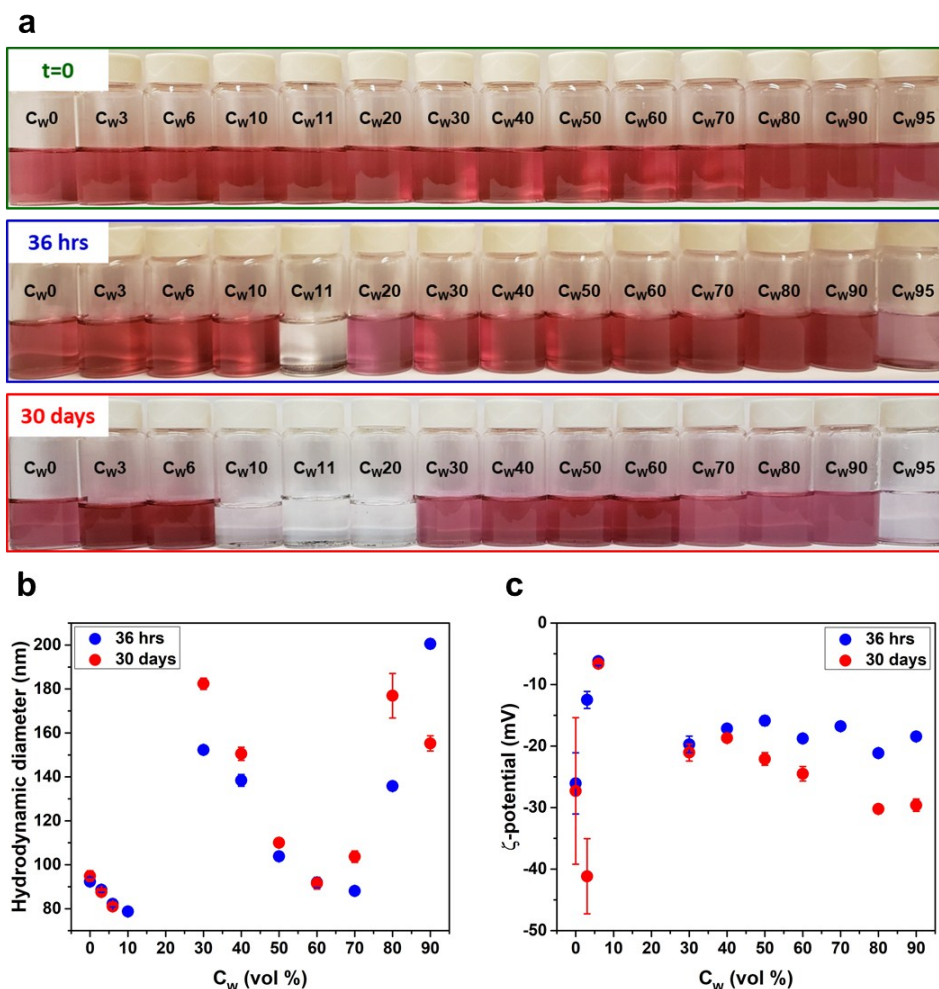
Fig. S1a shows the extinction spectrum of CTAB-functionalized AuNPs. The spectrum exhibits a strong peak centered at 524 nm, corresponding the localized surface plasmon resonance (LSPR) of the AuNPs. A weak peak centered at 750 nm was attributed to a small number of gold nanorods, typical for AuNP synthesis involving CTAB ligands.<sup>3</sup> The presence of gold nanorods had little effect on the colloidal stability and self-assembly behaviour reported in our work. Fig. S1b shows the TEM image of the CTAB-tethered AuNPs. The AuNPs have a spherical shape an average diameter of 24 nm (Fig. S1c).



**Fig. S1.** (a) Extinction spectrum of as-synthesized CTAB-capped AuNPs in water. (b) TEM image of CTAB/AuNPs. (c) Distribution of diameters of AuNPs, TEM image analysis.

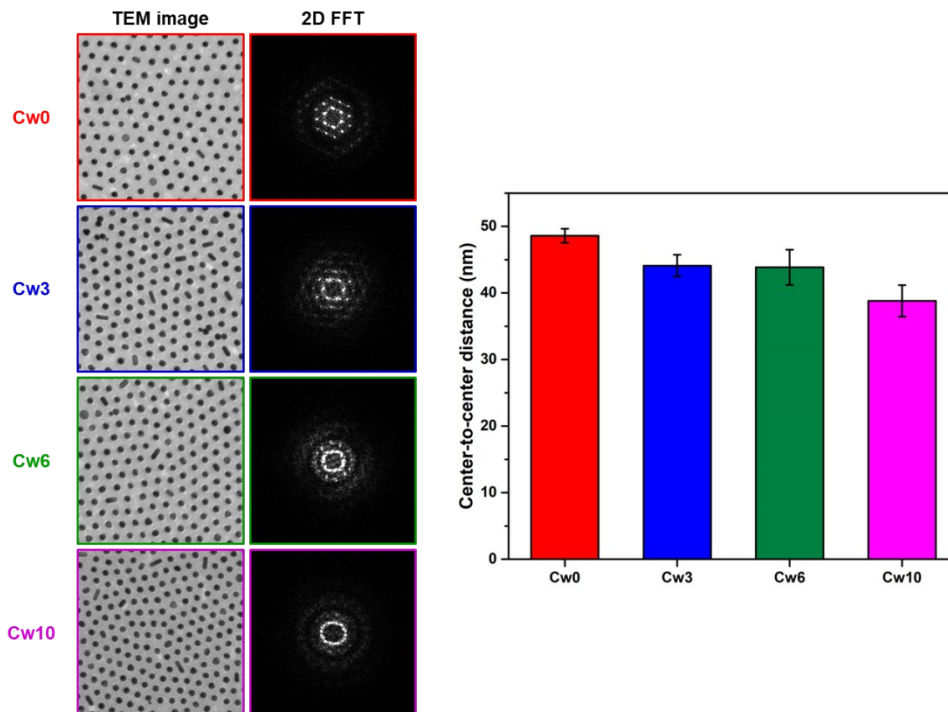
Fig. S2a shows solutions of CTAB/PS-capped AuNPs in water/THF mixtures with varying  $C_w$ , which were stored for different time intervals after addition of water. While little change in bright pink color of the colloidal solutions was observed immediately adding water, after 36 hrs, AuNP precipitation occurred at  $C_w=11$  vol% and, to a less degree, at  $C_w=95$  vol% (a slight change in colour of the solution occurred at  $C_w=20$  vol%). After 1 month, complete AuNP was observed at  $C_w=10-20$  vol% and  $C_w=95$  vol%. Despite some variation in the color, the rest of the colloidal solutions remained stable.

Fig. 2b and c shows the variation of hydrodynamic diameter ( $D_h$ ) and  $\zeta$ -potential, respectively, of CTAB/PS-tethered AuNPs, plotted as a function of following 36 hr and one month incubation. No significant change in  $D_h$  and  $\zeta$ -potential was over 1 month. In Fig. S2b, at  $30 < C_w < 90$  vol% large  $D_h$  values in the range of 90-200 nm corresponded to AuNP clusters, which became larger at  $C_w > 70$  vol%. Fig. S2c shows the CTAB/PS-tethered AuNPs gained a strong negative  $\zeta$ -potential of about -40 mV in THF. The addition of water initially caused the  $\zeta$ -potential to decrease to almost zero at  $C_w=10$  vol%, however for assemblies of CTAB/PS-capped AuNPs in solutions with  $30 < C_w < 90$  vol%, the value of  $\zeta$ -potential was in the range of -20 to -30 mV.



**Fig. S2.** (a) Photographs of the solutions of CTAB/PS-tethered AuNPs in water/THF mixtures with varying water content,  $C_w$ , taken 0, 36 hrs and 30 days after addition of water to the AuNPs solution in THF. (b, c) Variation in hydrodynamic diameter (b) and  $\zeta$ -potential (c) of AuNPs in water/THF mixtures 36 hrs and 30 days after adding water to AuNP solution in THF, plotted as a function of  $C_w$ .

The decrease in dimensions of CTAB/PS-functionalized AuNPs with increasing  $C_w$  at  $C_w < 10$  vol % was also observed in TEM images of dense AuNP arrays with a uniform interparticle spacing (determined by double thickness of the PS layer). As shown in Fig. S3, TEM images show a quasi-hexagonal arrangement of CTAB/PS-capped AuNPs at  $C_w$  of 0, 3, 6, and 10 vol %. The interparticle center-to-center distance decreased with increasing  $C_w$ , consistent with reducing solvent quality and stronger collapse of the PS layer.



**Fig. S3.** Left: TEM images of dense 2D arrays of CTAB/PS-functionalized AuNPs at  $C_w$  of 0, 3, 6 and 10 vol% and corresponding 2D FFT transform analysis of the images Right: Average center-to-center distance in the arrays of CTAB/PS-functionalized AuNPs (as in (a)).

The precipitate obtained in the solution of CTAB/PS-functionalized AuNPs at  $C_w=11$  vol % was collected and redispersed in THF. Upon adding water to this solution at varying  $C_w$ , the colloidal stability and self-assembly of the AuNPs was similar to that of the original colloidal solution (Fig. S4). More specifically, two precipitation regimes were observed after 1 month storage at  $C_w$  of 11-20 and 95 vol %. The above observed relationship between  $D_h$  and  $C_w$  was also observed for the stable solutions at other solvent compositions. In addition, the trend in variation of  $\zeta$ -potential vs.  $C_w$  was similar (except  $\zeta$ -potential being close to zero at  $C_w$  of 3 and 6 vol % after 36 hr and 1 month storage).

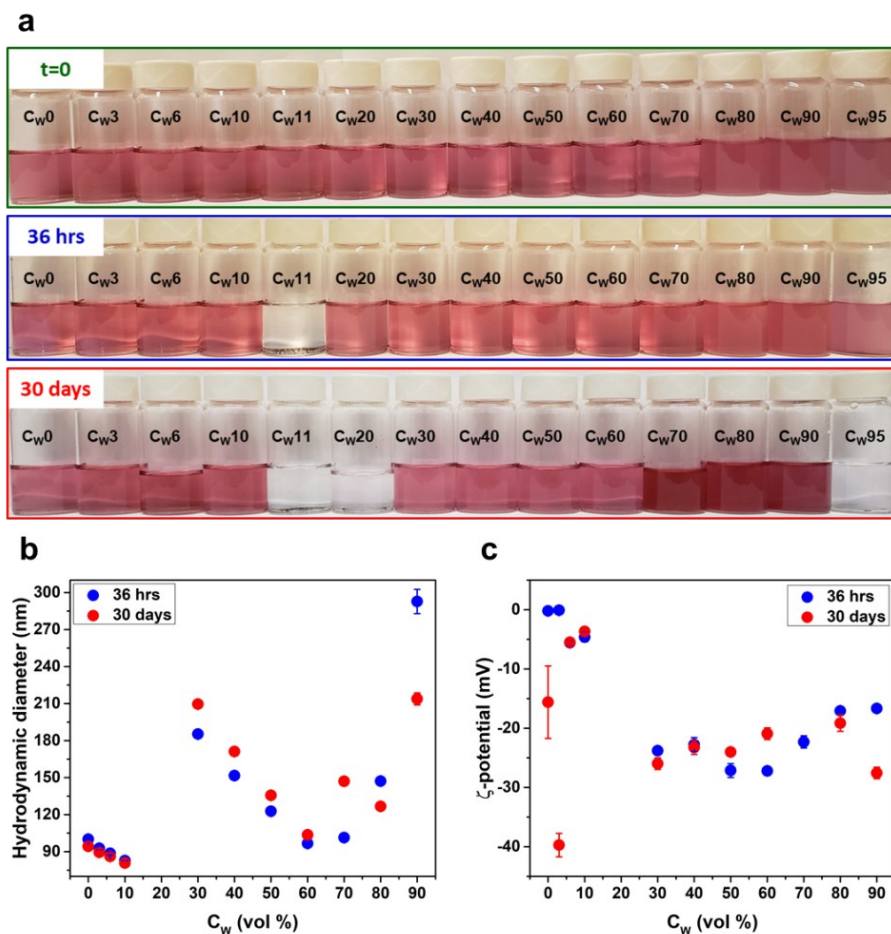


**Fig. S4.** (a) Photographs of the solutions of CTAB/PS-capped AuNPs in water/THF mixtures prepared by dissolving in THF the precipitate obtained at  $C_w=11$  vol% and the addition of water at various  $C_w$ . (b, c) Variation in hydrodynamic diameter (b) and  $\zeta$ -potential (c) of AuNPs as in (a), plotted as a function of  $C_w$ .

Fig. S5a illustrates the variation in colloidal stability of CTAB-stabilized AuNPs in water/THF mixtures with varying  $C_w$ . The addition of THF caused instant change in color of the colloidal solution at  $C_w$  in the range of 5-11 and 70-80 vol %. These changes were preserved after 1 month storage of CTAB-stabilized AuNP solutions. Fig. S5b shows that in water, the average hydrodynamic diameter  $D_h$  of CTAB-functionalized AuNPs was 32 nm. Larger  $D_h$  values indicated AuNP aggregation, which was the strongest at  $C_w$  of 11 and 70-80 vol %. No noticeable precipitation was observed for all colloidal solutions. Fig. S5c shows that  $\zeta$ -potential was positive and high at  $C_w > 90$  vol%, close-to-zero at  $C_w = 70-80$  vol%, and negative at  $C_w < 60$  vol%.



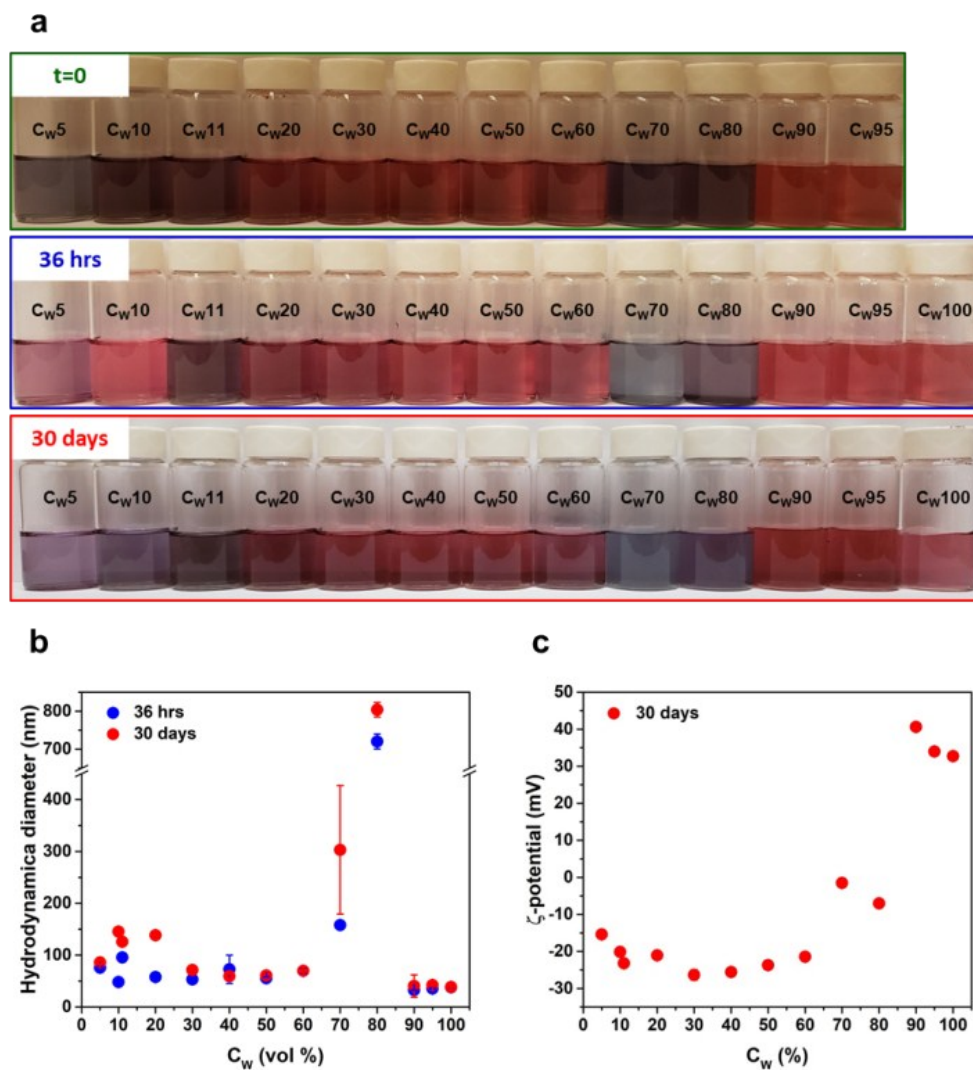


**Fig. S5.** (a) Photographs of the solution of CTAB-stabilized AuNPs in water/THF solutions with varying water content,  $C_w$ , following 0, 36 hrs and 30 day incubation after addition of THF to the solution of AuNPs in water. (b, c) Variation in hydrodynamic diameter (b) and  $\zeta$ -potential (c) of CTAB-functionalized AuNPs in water/THF mixtures (as in (a)), plotted as a function of  $C_w$ .

Fig. S6 compares the normalized spectra of AuNPs in a unimer state at  $C_w$  of 3-10 vol% and AuNPs in a cluster state at  $C_w$  of 30-70 vol %. A notable redshift was observed for AuNP clusters, due to a strong plasmonic coupling of individual AuNPs and the change in the dielectric constant of the AuNP environment (the refractive indexes of THF, water and PS are  $\sim 1.4$ , 1.33, 1.6, respectively). The LSPR peak intensity was lower for AuNP clusters, due to the stronger scattering.



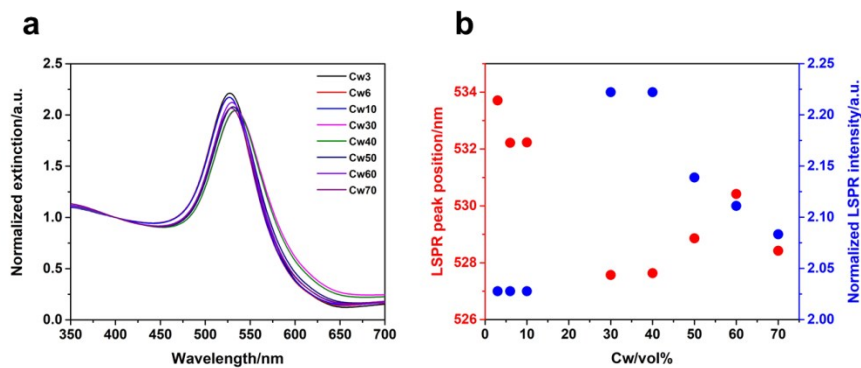


**Fig. S6.** (a) UV-vis extinction spectra of CTAB/PS-capped AuNPs in the THF/water mixtures with varying  $C_w$ , after normalization against the intensity at 400 nm. (b) Variation in  $\lambda_{LSPR}$  position (red) and intensity (blue), plotted against  $C_w$ .

## References

1. R. M. Choueiri et al. *Nature* 2016, 538, 79.
2. E. Galati, E.; H. Tao, C. Rossner, E. B. Zhulina, and E. Kumacheva, E. *ACS Nano* 2020, <https://doi.org/10.1021/acsnano.0c00108>
3. L. Scarabelli, A. Sánchez-Iglesias, J. Pérez-Juste and L. M. Liz-Marzán. *J. Phys. Chem. Lett.* 2015, 6, 4270.